ORIGINAL PAPER

Construction of a novel Cu(II)-selective electrode with long life span based on 8-aminoquinoline functionalized bentonite

Bilge Dogan[1] · Fatih Coldur[2] · Bulent Caglar[2] · Agah Oktay Ozdemir[3] · Eda Keles Guner[4] · Kemal Volkan Ozdokur[2]

Abstract
A novel 8-aminoquinoline-functionalized bentonite was utilized as an electroactive sensing element in the construction of a potentiometric carboxylated-PVC-based polymeric membrane electrode. The electrode exhibited a linear response for copper(II) ions in the concentration range of $1.0 \times 10^{-5} - 1.0 \times 10^{-2}$ mol/dm^3 with a slope of 28.24 mV/decade. While the response time of the electrode determined as about 20 s, its detection limit and long life time was determined as 5.0×10^{-6} mol/dm^3 and 5 months, respectively. The proposed electrode was applied for the potentiometric detection of Cu(II) contents of some spiked water samples and satisfied results were attained.

Graphical abstract
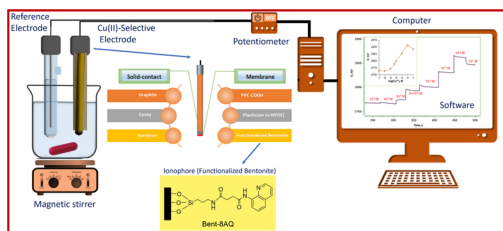
✉ Fatih Coldur
fatihcoldur@hotmail.com

✉ Bulent Caglar
bcaglar55@gmail.com

1 Department of Chemistry, Institute of Science and Technology, Erzincan Binali Yildirim University, 24030 Erzincan, Turkey

2 Department of Chemistry, Faculty of Arts and Sciences, Erzincan Binali Yildirim University, 24100 Erzincan, Turkey

3 Department of Design, Vocational School, Erzincan Binali Yildirim University, 24100 Erzincan, Turkey

4 Department of Property Protection and Security, Uzumlu Vocational School, Erzincan Binali Yildirim University, 24150 Erzincan, Turkey

Introduction

Copper is considered the third most abundant heavy metal on earth after Fe and Zn and is found at low levels in water, rocks, and crust [1]. Copper is commonly used in many industries such as wiring, electrodeposition, painting, metal processing, fertilizers, wood, pigment industries, etc., because of its distinct properties which include high electrical conductivity, flexibility, chemical stability, and the ability to alloy with a wide range of metals [2, 3]. As a result of copper-based human activities on the world, the release of this element into the environment increases day by day.

As a micronutrient, copper is essential for the normal functioning of living organisms [4]. It participates in many physiological processes and the synthesis of neuropeptides, has immune functions and serves as a cofactor for many redox enzymes [5]. However, when its level is over

the appropriate quantity in the living things, it shows toxic and harmful impact on health. High levels of copper can cause several illnesses such as Alzheimer's disease, Wilson's disease, depression, bipolar disorder, stomach convulsions, hypothyroidism, Hashimoto's disease, infertility, vomiting, memory loss, premenstrual syndrome, gastrointestinal disorders, liver and kidney damage, pelvic inflammatory disease [6, 7].

Managing the state of the natural environment such as soil, sewage, and water samples has been recently one of the momentous environmental issues due to its effects on the human and other living organisms. The most harmful aspect of copper as one of the most significant water pollutant emerged from that the tolerance limit for copper in drinking water is 1.3 mg/dm^3 according to World Health Organization (WHO) guidelines [8]. Therefore, it is extremely vital to monitor copper concentrations in different water samples and necessary to develop a simple, reliable and inexpensive technique for the determinations.

Up to date, several methods, involving Atomic Absorption Spectrometry (AAS) [9], Graphite Furnace Atomic Absorption Spectrophotometry (GF-AAS) [10], Flame Atomic Absorption Spectrometry (FAAS) [11], Electrothermal Atomic Absorption Spectrometry (ET-AAS) [12], neutron activation analysis [13], X-ray fluorescence [14], fluorimetry [15], Inductively Coupled Plasma-Mass Spectrometry (ICP-MS) [16], Inductively Coupled Plasma-Optical Emission Spectrometry (ICP-OES) [17], Liquid–Liquid Micro extraction-UV–vis Spectrophotometry (LLM-UVVS) [18], Capillary Electrophoresis (CE) [19], chromatography [20], gravimetric detection [21], Adsorption Stripping Voltammetry (ASV) [22], and potentiometry [23, 24] have been introduced for the determination of copper(II) ions. While most of these methods have many advantages, such as reduced detection limits and enhanced sensitivity, they also have some limitations including, incorporation of expensive and sophisticated equipment, need for skilled personnel and special pre-treatment processes for the sample, complex measurement procedures and long detection periods. Therefore, the development of reliable, simple, and inexpensive methods for copper measurement is of great interest.

Potentiometry is one of the most commonly used electrochemical methods for the quantitative measurement of various metal ions. In recent years, ion-selective potentiometric electrodes have been used in many fields for the identification of different species as an alternative to the aforementioned costly detection methods due to their advantages, such as high selectivity, wide dynamic range, low detection limit, low cost, short analysis time, high accuracy and precision, simple design, no damage to the measuring material, mostly no pre-treatment step, determination even in colored and turbid solutions [25].

Although various types of ion-selective electrodes presented in the literature, ionophore-based PVC-membrane electrodes have been the most broadly manufactured types among the other ISE types in the field of potentiometry. As well-known, the most important ingredient that imparts selectivity and sensitivity to a PVC-membrane electrode is the electroactive component, also known as ionophore. In PVC-membrane electrodes, the ionophore material and other membrane components are physically brought together and the ionophore material is embedded in the matrix without a chemical bonding (chemical interaction). The resulting membrane is then coated on the surface of an ion to electron transducer as a thin film. However, one of the most important problems encountered in this type of solvent polymeric PVC-membrane electrodes is the dissolution of the membrane components and leakage into the measurement solution over time [26]. Therefore, the deteriorations in the potentiometric performance properties of the electrodes such as detection limit, life-time selectivity, sensitivity, stability, etc. are observed as the day passes [27, 28]. To overcome this problem, a material either chemically modified with ionophore or with functional groups displaying ionophore properties can be included in the membrane structure, which does not leach into the measuring solution [29, 30]. Alternatively, modified materials that have functional groups and complexing sites in appropriate orientation and directions complementary to the target species, thus creating selective and sensitive interactions with the target species, can be used directly as an electroactive sensing component in the PVC matrix [31–33].

In the current research, we have executed the chemical functionalization of a bentonite. The structural description of the resulting material was achieved using powder X-ray diffraction (XRD), Fourier-transform infrared spectroscopy (FT-IR), and scanning electron microscopy-energy, dispersive X-ray spectroscopy (SEM–EDX) techniques. The obtained material was implemented as an electroactive substance in the fabrication of a solid-contact carboxylated-PVC-membrane electrode selective to Cu(II) ions. The analytical performance characteristics of the suggested electrode were appointed. The analytical application of the electrode were carried out using the electrode for the determinations of Cu(II) contents of spiked water samples.

Results and discussion

Characterization of the samples

The XRD patterns of Bent and Bent-8AQ composite are displayed in Fig. 1a, b, respectively. (001), (020–110), (130–200) and (060) diffractions of bentonite are observed at 7.04°, 20.31°, 36.89°, and 61.81° (2θ) with the distances
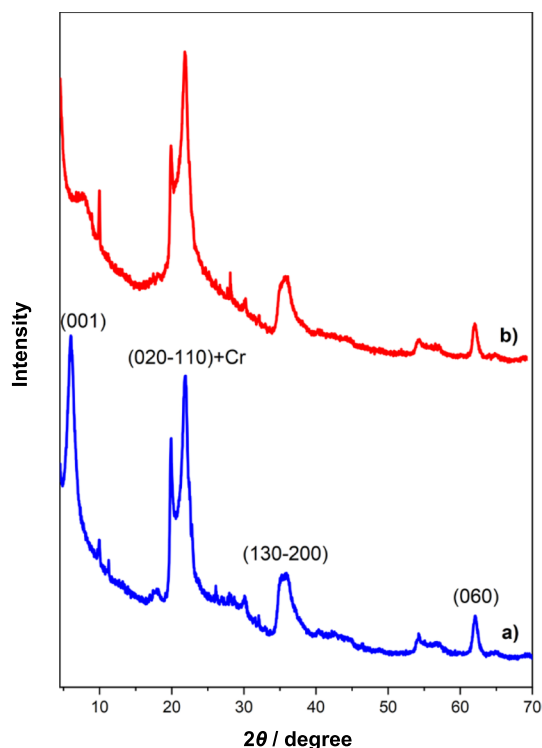
Fig. 1 XRD patterns of **a** Bent and **b** Bent-8AQ composite

Fig. 2 FT-IR spectra of **a** Bent and **b** Bent-8AQ composite

of 13.44, 4.37, 2.43, and 1.50 Å, respectively, and signifies that the main component of the Bent is montmorillonite [34]. The peaks belonging to cristobalite (Cr) are also seen at 22.16° and 27.17° (2θ). In addition, (060) diffraction has 1.50 Å value showing that the bentonite contains a dioctahedral montmorillonite [34, 35]. After the grafting of 8AQ onto bentonite by consecutive synthesis process, the intensity of (001) peak is significantly decreased and widen due to the delamination of bentonite layers by incorporation of 8AQ and/or used chemicals during synthesis [36, 37]. However, the positions of the other diffractions peaks belonging to bentonite did not change after the grafting process. This situation showed that 8AQ molecules are grafted on delaminated clay layers.

FT-IR spectroscopy was used to confirm the existence of grafted 8AQ species and the comparative FT-IR spectra of Bent and Bent-8AQ composite are shown in Fig. 2a, b. The IR peaks at 3619 and 917 cm^{-1} are attributed to the stretching and bending vibrations of structural hydroxyls in octahedral layers, respectively, while the IR band at 3406 and 1635 cm^{-1} are ascribed to hydroxyl stretching and bending vibrations of adsorbed water species on bentonite, respectively (Fig. 2a). The strong IR band at 1007 cm^{-1} belongs to the Si–O–Si stretching and the IR bands 524, 448, and 424 cm^{-1} are correspond to Si–O, Al–O–Si, and Si–O–Si bending, respectively [34–36].
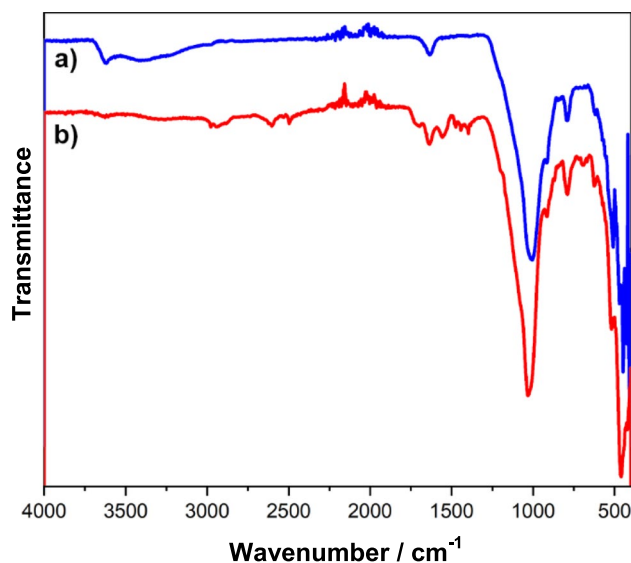
Furthermore, a peak is seen at 790 cm^{-1} which is related to cristobalite as confirm by XRD. The grafting of 8AQ on bentonite by consecutive synthesis process resulted in appearance the novel IR vibration peaks for Bent-8AQ composite. The IR bands in the region 2972–2885 cm^{-1} correspond to stretching vibration of CH_2 groups whereas the weak peak at 3018 cm^{-1} assigned to the aromatic C-H stretching vibrations. The new IR bands 1712, 1557, and 698 cm^{-1} originating from C=O stretching, N–H bending, and aromatic C-H deformations, respectively, confirming the chemical binging of 8AQ to Bent-COOH via amidation reaction.

SEM images and EDX figures of Bent and Bent-8AQ composite are presented in Fig. 3. The SEM images showed that there are some differences morphologies of Bent and Bent-8AQ composite as it presented in Fig. 3a, b, respectively. The SEM image of Bent reveals curved plates with fluffy appearance and porous structure whereas the SEM image Bent-8AQ composite has more smooth surface and compact appearance by grafting of 8AQ. In addition, the EDX analysis of Bent indicates that bentonite contains O (51.68 wt%), Si (33.33 wt%), Al (10.57 wt%), Fe (1.36 wt%), Mg (2.49 wt%), Ca (0.54 wt%), and Na (0.03 wt%) which are characteristic constituents of clay minerals (Fig. 3c). However, the Bent-8AQ composite contains O (44.97 wt%), Si (20.10 wt%), Al (4.20 wt%), Fe (0.39 wt%), Mg (0.93 wt%), Ca (0.39 wt%), Cl (1.33 wt%), C (22.90 wt%), and N (4.79 wt%) (Fig. 3d). Si, Al, Fe, O, Mg, and Ca atoms were related to Bent clay whereas C and N atoms were originated from production of Bent-8AQ composite (Fig. 3d).

Fig. 3 SEM images of **a** Bent and **b** Bent-8AQ composite, EDX spectra of **c** Bent and **d** Bent-8AQ composite
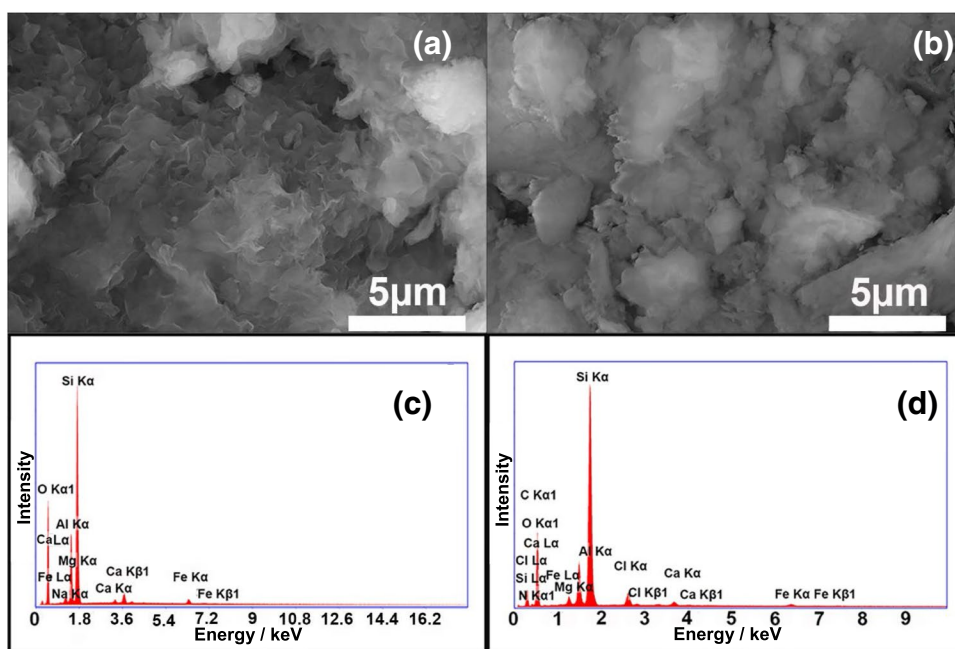

Potentiometric performance characteristics of the proposed electrode

Preliminary measurements of the prepared electrode showed that the electrode had a more selective potentiometric behavior towards Cu(II) ions. Therefore, potentiometric measurements were taken in a series of Cu(II) whose concentrations ranging from 10^{-1} to 10^{-7} mol/dm^3 to determine the linear working range, detection limit and sensitivity (slope) of the electrode. The observed measurements and the response curve corresponding to these measurements are illustrated in the Fig. 4. The suggested electrode exhibited a linear response to Cu(II) ions in the concentration range of 10^{-2} – 10^{-5} mol/dm^3 ($R^2 = 0.9991$) with the slope of 28,24 mV decade^{-1} (Fig. 5). The detection limit of the electrode was calculated from the intersection of the two extrapolated linear part of the response curve as 5×10^{-6} mol/dm^3 according to IUPAC recommendations [38].

Response time refers to the time elapsed from the immersion moment of the electrode into the measuring solution until the equilibrium potential is reached. Response time of an ion-selective electrode, as with other types of sensors, is

Fig. 4 The potentiometric response of the electrode to Cu(II) solutions at various concentrations and corresponding response curve (inset)
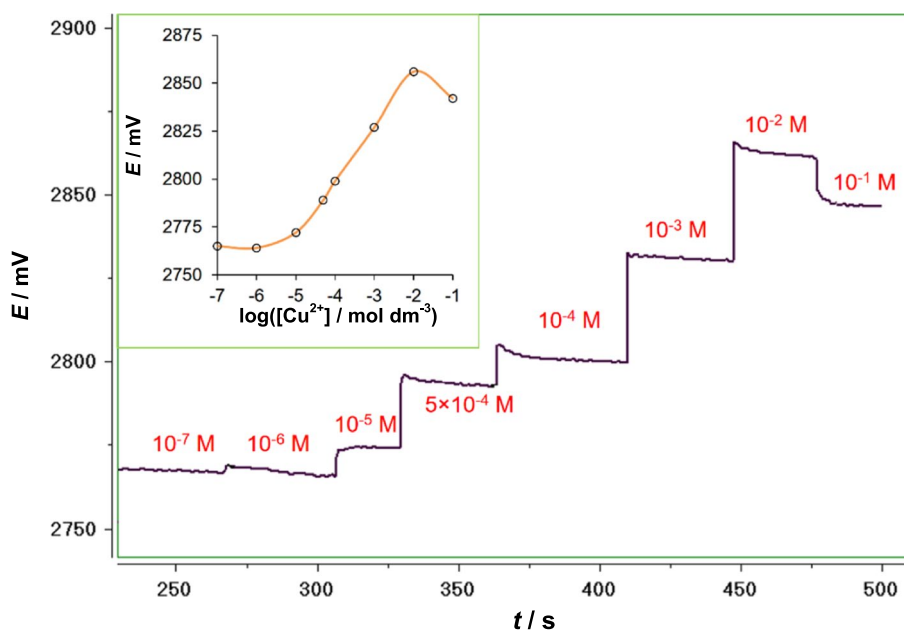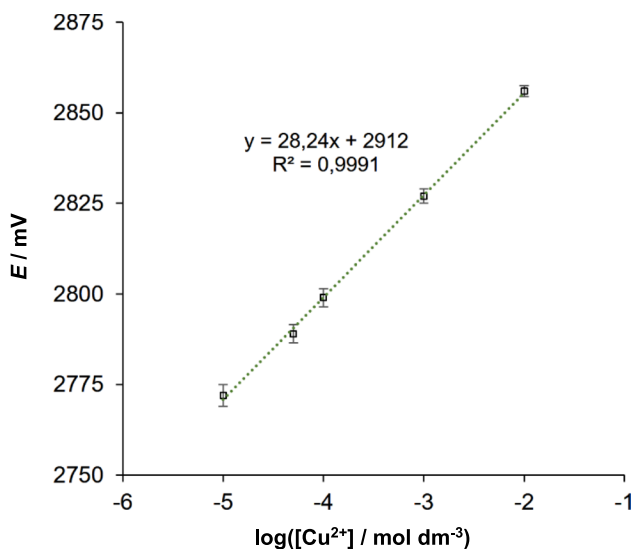
Fig. 5 The calibration plot of the electrode constructed in the linear response region

a significant task for analytical applications. Response time of an ion-selective electrode alters depending on electrode type, conditioning solution, measured concentration range, degree of concentration change, the amount of interferences, and measurement direction.

For the determination of average response time of the current electrode, the responses of the electrode in Cu(II) solutions in the concentration range of $10^{-2}-10^{-5}$ mol/dm^3 were recorded from low to high concentration and vice-versa depending on the time that elapsed while the measurement

solutions were continuously blended. The regarding records were illustrated in Fig. 6. The time required for potential stabilization following each concentration change was calculated as t_{95} [38]. The average of the time periods for each concentration change was denoted as response time of the electrode. As can be seen, the response of the electrode to Cu(II) ions is satisfactorily rapid (≈ 20 s). This fact confirms the presence of a rapid equilibrium between the aqueous phase and membrane phase.

To conceive the repeatability of the proposed Cu(II)-selective electrode, successive measurements were carried out in 10^{-4}, 10^{-3}, and 10^{-2} mol/dm^3 Cu(II) solutions. The acquired potential measurements are displayed in Fig. 7. The average and standard deviation values of the measured potentials for 10^{-4}, 10^{-3}, and 10^{-2} mol/dm^3 Cu(II) solutions were calculated as 2784.9 ± 0.8, 2814.0 ± 0.8, and 2843.2 ± 0.6 mV, respectively.

The general potentiometric responses of the proposed electrode in Cu(II) solutions at various concentrations ($10^{-1}-10^{-7}$ mol/dm^3) and some foreign ion solutions at 10^{-2} mol/dm^3 were displayed in Figs. 8 and 9. As can be seen from Figs. 8 and 9, the response of the electrode to Cu(II) ions differs significantly from the response to other species and the electrode shows a selective behavior towards Cu(II) ions. The degree of selectivity of an electrode is expressed quantitatively by selectivity coefficients. The magnitude of the potentiometric selectivity coefficient describes the capability of an ISE to discriminate the primary ion from the interfering ion present in the measured solution. In the present research, separate solution method ($E_A = E_B$) [39] was operated for the calculation of selectivity coefficients

Fig. 6 The real-time response plot of the electrode depending on various Cu(II) solutions at different concentrations
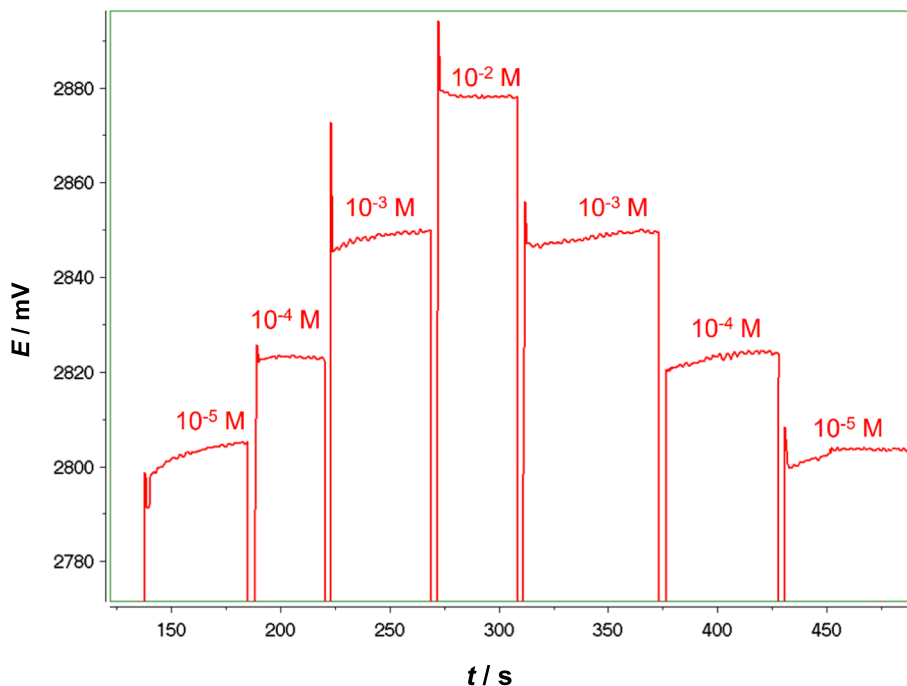
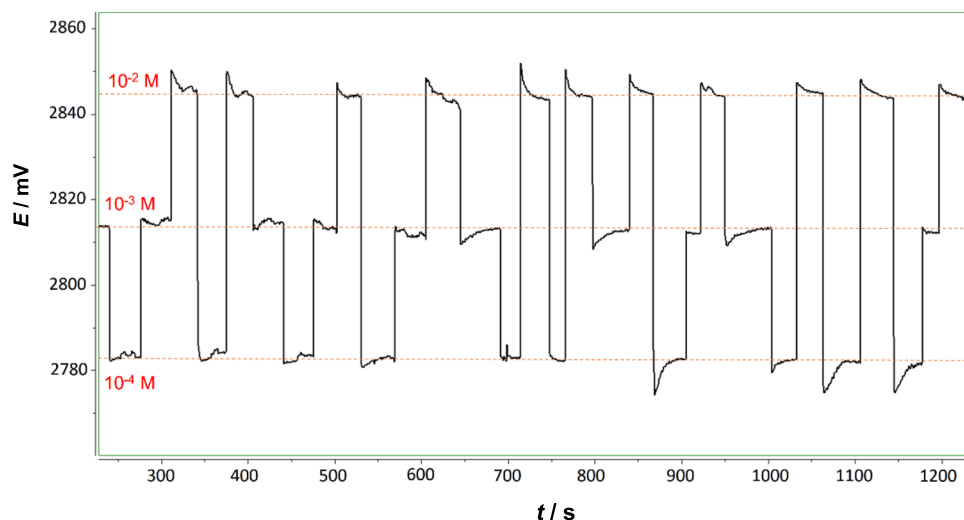**Fig. 7** Repeatability of the suggested Cu(II)-selective electrode

Fig. 8 Recorded potentiometric responses of the proposed electrode in the solutions of Cu(II) at various concentrations and in 10^{-2} mol/dm^3 solutions of studied interference species: (1) Na$^+$; (2) K$^+$; (3) NH$_4^+$; (4) Mg^{2+}; (5) Ca^{2+}; (6) Ba^{2+}; (7) Pb^{2+}; (8) Zn^{2+}

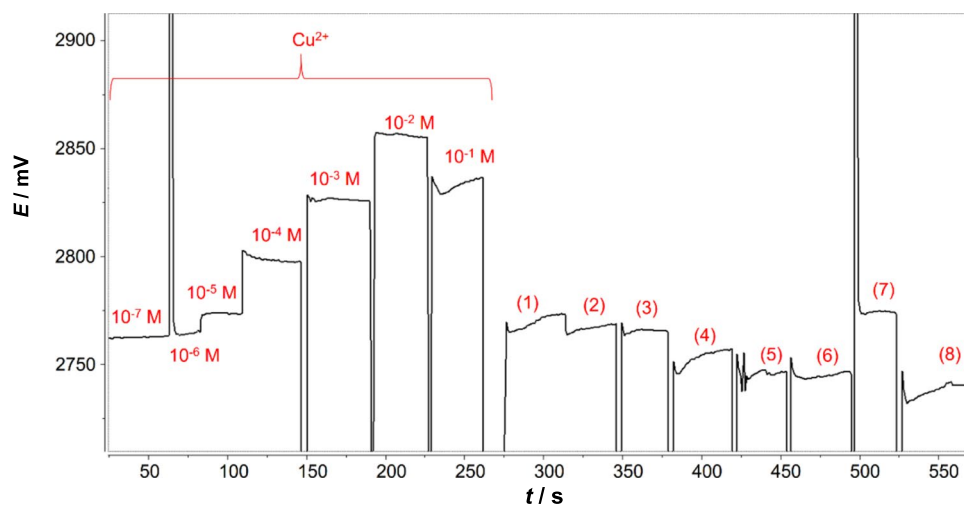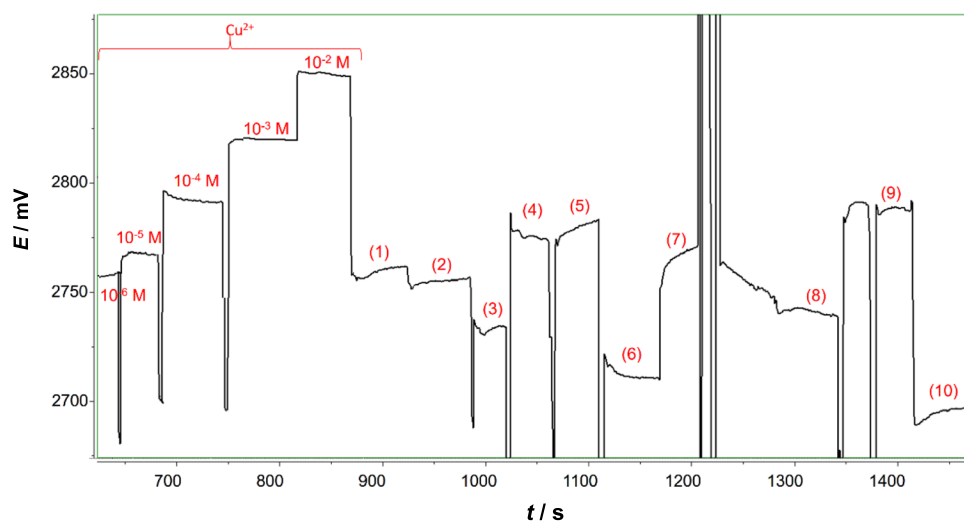**Fig. 9** Recorded potentiometric responses of the proposed electrode in the solutions of Cu(II) at various concentrations and in 10^{-2} mol/dm^3 solutions of studied interference species (1) Cd^{2+}; (2) Co^{2+}; (3) Ni^{2+}; (4) Al^{3+}; (5) Cr^{3+}; (6) Mn^{2+}; (7) Hg^{2+}; (8) fructose; (9) maltose; (10) L-alanine

for studied interferent species. In the calculation of the selectivity coefficients, the potential values measured in 1.0×10^{-2} mol/dm^3 solutions of the interfering ions were attained and these values were employed for the calculations of regarding Cu(II) concentrations from the linear equation of the calibration plot constructed for Cu(II) ions. The calculated Cu(II) ion concentration values and 1.0×10^{-2} mol/dm^3 concentration values of the interferents were inserted into the equation used to calculate selectivity coefficients, and thus the electrode's selectivity coefficients were determined for each interferent. The calculated selectivity coefficients are represented in Table 1. The attained selectivity coefficients point out that the electrode has reasonable selectivity for Cu(II) ions compared to the studied interferents. It can be said that this selective behavior of the membrane against Cu(II) ions is due to the formation of strong and selective interaction between Cu(II) ions and membrane structure, as a result of the synergistic effect emerged from the functionalized bentonite equipped with functional groups in appropriate positions and orientations, and the components

**Table 1** Selectivity coefficients ($K_{A, B}$) of the present Cu(II)-selective electrode calculated according to SSM

Species	Log $K_{A,B}$	Species	Log $K_{A,B}$
Na$^+$	− 2.92	Co^{2+}	− 3.31
K$^+$	− 3.06	Ni^{2+}	− 4.09
NH$_4^+$	− 3.21	Al^{3+-}	− 3,34
Mg^{2+}	− 3.52	Cr^{3+}	− 3,06
Ca^{2+}	− 3.88	Mn^{2+}	− 4.90
Ba^{2+}	− 3.84	Hg^{2+-}	− 2.82
Pb^{2+}	− 2,89	Fructose	− 3,88
Zn^{2+}	− 4.09	Maltose	− 2.21
Cd^{2+}	− 3.10	L-Alanine	− 5.40

of the membrane structure (plasticizer, carboxylated-PVC, ionic additive). In addition the interference effects of the Ag(I), Fe(II), and Fe(III) ions were also studied. However, the selectivity coefficients of the electrode against these ions could not be determined properly due to the disruptive effects of these ions on the electrode response.

The magnitude of the potential drift that occurred over time depending on the immersion time of the electrode in the solution was also investigated. For this purpose, the potential change was monitored by immersing the electrode in 10^{-3} and 10^{-4} mol/dm^3 Cu(II) solutions for about 2 h (Fig. 10). The drift values of 0.63 and 3.66 mV h^{-1} in the electrode potential was observed in 10^{-3} and 10^{-4} mol/dm^3 Cu(II) solutions, respectively. In both solutions, the observed noises of the signals were less than 1.0 mV. This results indicate that the electrode response is highly stable.

The pH profile of the suggested Cu(II)-selective electrode was examined to determine the proper pH operating range of the electrode. The influence of pH on the Cu(II)-selective electrode response was studied by recording potential values of 1.0×10^{-3} and 1.0×10^{-4} mol/dm^3 Cu(II) solutions at various pH values (2.0–12.0). Small amounts of hydrochloric acid (0.1 mol/dm^3) or sodium hydroxide solution (0.1 mol/dm^3) was added drop wise to adjust the solution pH to desired values between 2.0 and 12.0. Figure 11 illustrates the attained pH profile for the electrode. From Fig. 11, it can be seen that the recorded potential values obtained as a function of pH altered very slightly in the presence of constant 1.0×10^{-3} and 1.0×10^{-4} mol/dm^3 Cu(II) solutions in the pH range 4.2–7.7. In this pH range, the electrode is not thrilled by the pH of the measurement medium, so the pH operating range of the electrode can be assumed to be 4.2 to 7.7. Above the pH = 7.7, the electrode potential begins to drop rapidly. This is presumably due to the complexation of Cu(II) ions with the gradually increased OH$^-$ ion

Fig. 10 The observed noise and drift in the recorded Cu(II)-selective electrode response depending on time in 10^{-3} and 10^{-4} mol/dm^3 Cu(II) solutions
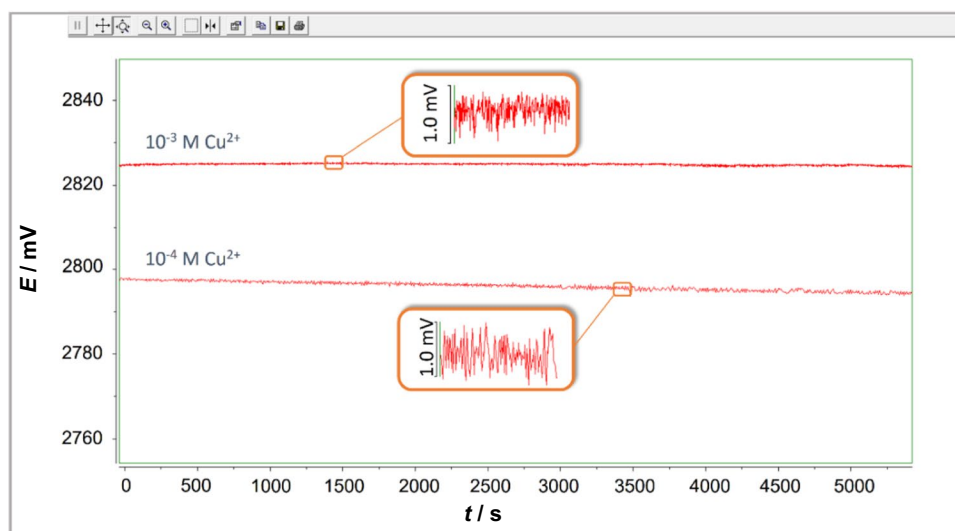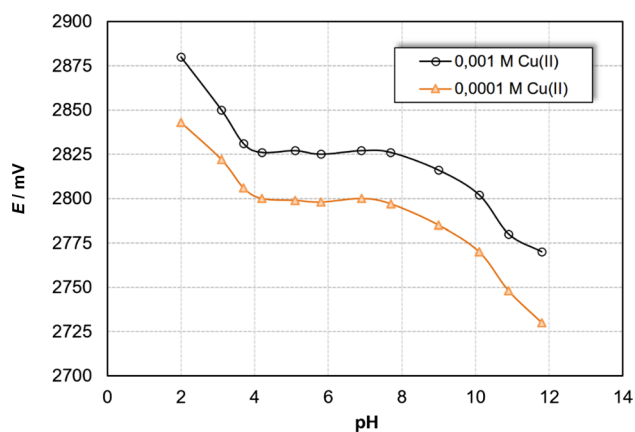
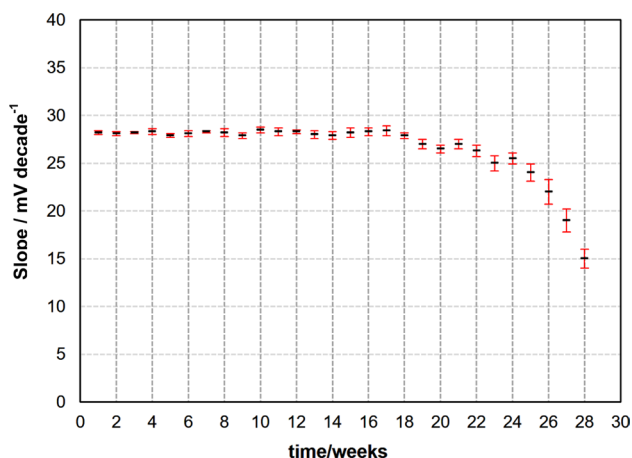Fig. 11 The pH profiles of the presented electrode in 10^{-3} and 10^{-4} mol/dm^3 Cu(II) solutions

Fig. 12 İnvestigation of the life time of the introduced Cu(II)-selective electrode

concentrations depending on pH. We think that the increase in the potential values observed in pHs lower than 4.2 is on account of the interference effect of increased H$_3$O$^+$ ion concentrations. In the pHs lower than 4.2, the electrode begins to respond H$_3$O$^+$ ions as well as Cu(II) ions.

The lifetime of the electrode was evaluated by taking weekly measurements by the electrode in standard Cu(II)

solutions and monitoring the emerged changes in the electrode slope. For this purpose, using a freshly prepared electrode, three calibration lines were created with standard calibration solutions after conditioning in 0.001 mol/dm^3 Cu(II) solution for half an hour before each weekly study. The obtained mean slope values of these lines for each week with their error bars (as standard deviation type) were plotted over time (Fig. 12). As can be seen from Fig. 12, after a long period of time (22 weeks), no significant decrease was observed in the slope of the electrode's calibration line. However, at the end of this period, a slow decline in the slope of the electrode was observed at first, and it was observed that this slope decrease accelerated after the 25th week. Similarly, as time progresses, the standard deviations of the slope values also increase. According to these results, it can be stated that the lifetime of the electrode is around 5 months. These findings show that the lifetime of the electrode is much longer when compared to the classical neutral ionophore-based PVC membrane ion-selective electrodes available in the literature, which have an average lifetime of 2–3 months.

Analytical application of the proposed electrode

To evaluate the analytical applicability of the presented Cu(II) selective electrode, Cu(II) contents of some spiked tap water samples was determined via potentiometric measurements. Thus, water samples (pH = 5) were prepared in which known amounts of Cu(II) were spiked to coincide with the linear working range of the electrode, and each water sample was analyzed in terms of Cu(II) content by standard addition method. The obtained results were given in Table 2. As can be seen, the recovery of the suggested electrode for spiked samples was in the range of 99.5–102.0% with the RSDs below 3.92%. The two-tailed Student's t test indicated that the experimental t values for all the studied water samples at 95% confidence level were less than the theoretical t value (2.57) for 5 replicates. These calculated t values indicate that the potentiometrically estimated Cu(II) levels are statistically well-matched with the known levels of Cu(II) in the spiked water samples and there is no discernible difference between them at the relevant confidence level.

Table 2 Potentiometric determination of Cu(II) contents of spiked water samples	Water sample	Expected Cu(II) content/mmol dm^{-3}	Found average Cu(II)content/mmol dm^{-3} ($N=5$)	RSD/%	t test $t_{experimental}$[a]	Recovery/%
	1	0.050	0.051	3.92	1.11	102.0
	2	0.100	0.101	3.76	0.39	100.7
	3	0.500	0.498	1.06	0.85	99.6
	4	1.000	0.997	2.53	0.30	99.7
	5	2.000	1.990	1.33	0.85	99.5

[a]$t_{theoretical}=2.57$ at 95.0% confidence interval for two-tailed Student's t test

Consequently, we can express that the current ion-selective electrode can be simply and satisfactorily applied for the determination of Cu(II) contents of specimens.

Conclusion

In the current study, chemical modification of a bentonite with 8-aminoquinoline was revealed for the first time and its characterization was performed. The potentiometric applicability of the resultant material as an electroactive substance was investigated. On the basis of the presented results, 8-aminoquinoline functionalized bentonite structure obtained by chemical modification can be regarded as an electroactive sensing element for the construction of a carboxylated-PVC membrane-based Cu(II)-selective potentiometric electrode. The proposed electrode has been shown to have good operating characteristics (ease of preparation, high life span, short response time, low detection limit, wide linear range, long-term stability, low cost, Nernstian behavior, and satisfied selectivity) and advantages over the high-cost sophisticated alternative detection methods. The developed Cu(II)-selective electrode was successfully employed for the determination of Cu(II) contents of spiked water samples. Some characteristic features of the proposed sensor are summarized in the Table 3 in comparison with some copper(II) selective potentiometric sensors available in the literature [40–47]. The long life time of the proposed electrode emerged from the chemical modification, is quite remarkable when compared to conventional neutral ionophore-based polymeric membrane electrodes. This feature can provide significant advantages, especially, for fluidic media measurements that necessitate sensor with higher signal stability and longer life time. The present study has shown that the approach applied here can be used in the future to develop potentiometric polymeric membrane electrodes exhibiting selective response to various species by utilizing such materials chemically modified with different appropriate chemical species.

Experimental

The bentonite utilized as starting material for the functionalized bentonite material was Unye bentonite which is an important mineral resource in Turkey. (3-Aminopropyl)-triethoxysilane (APTES), triethylamine (TEA, Et3N), succinic anhydride, ethyl chloroformate (EtOCOCl), 8-aminoquinoline (8AQ), toluene, 1,4-dioxane, tetrahydrofuran (THF), carboxylated poly(vinyl chloride) (PVC-COOH) (5% carboxyl basis), *o*-nitrophenyloctylether (*o*-NPOE) were obtained from Sigma-Aldrich (Germany). The epoxy (TP3100) and hardener (Desmodur RFE) used in solid-contact preparation were obtained from Denlaks (Turkey) and Bayer (Germany) companies, respectively. All chemicals used for the preparation of the solutions throughout this study were at analytical grade obtained from Sigma-Aldrich (Germany). Deionized water (18.3 MΩ) employed in the study was obtained from the Human Corporation Zeener Power II (Korea) water purification system. XRD patterns were obtained on a PANalytical Empyrean diffractometer using Ni filtered CuKα radition ($\lambda = 1.54050$ Å; 45 kV and 40 mA) at ambient temperatures. FT-IR spectra of samples were recorded on Thermo Nicolet 6700 Fourier-transform infrared (FT-IR) spectrometer in the region 4000–400 cm^{-1}. The SEM images and EDX data were taken using FEI QUANTA 450 Field Emission Scanning Electron Microscopy. All potentiometric measurements were conducted using a laboratory-made computer-controlled potentiometric measurement system. A Gamry (USA) brand saturated Ag/AgCl electrode was used as reference electrode in all potential measurements. All pH measurements were carried

Table 3 Comparison of the some potentiometric characteristics of the suggested Cu(II)-selective sensor with the reported electrodes

Sensor	Linear range/mol dm^{-3}	Detection limit/mol dm^{-3}	Slope/mV decade^{-1}	Response time/s	pH range	Lifetime/months	References
1	10^{-4}–10^{-2}	4.4×10^{-6}	37.5	0.25	2–6	3	[40]
2-a	5×10^{-4}–5×10^{-2}	4×10^{-4}	29.9	5–10	2.5–5.0	1.5	[41]
2-b	5×10^{-4}–10^{-1}	4×10^{-4}	29.7	5–10	3.2–4.7	1.5	
2-c	1×10^{-6}–1×10^{-2}	2×10^{-7}	30.0	5–10	4.0–5.0	1.5	
3	1.78×10^{-5}–1.00×10^{-1}	1.78×10^{-5}	50.0	‘30	3.0–6.0	–	[42]
4	8.1×10^{-6}–1.0×10^{-2}	7.4×10^{-6}	34.2	‘20	4.5–6.0	2	[43]
5	5.0×10^{-6}–1.6×10^{-2}	2.0×10^{-6}	29.2	‘10	4–6	2	[44]
6	1×10^{-5}–1×10^{-1}	2.0×10^{-6}	28.1	22	3–8	2	[45]
7	9.8×10^{-6}–1.0×10^{-1}	–	30.3	20	3.1–7.6	2	[46]
8	5.0×10^{-6}–1.0×10^{-1}	4.7×10^{-6}	29.6	‘30	1.9–5.2	> 5	[47]
9	1.0×10^{-5}–1.0×10^{-2}	5.0×10^{-6}	28.2	‘20	4.2–7.7	5	This work

Scheme 1
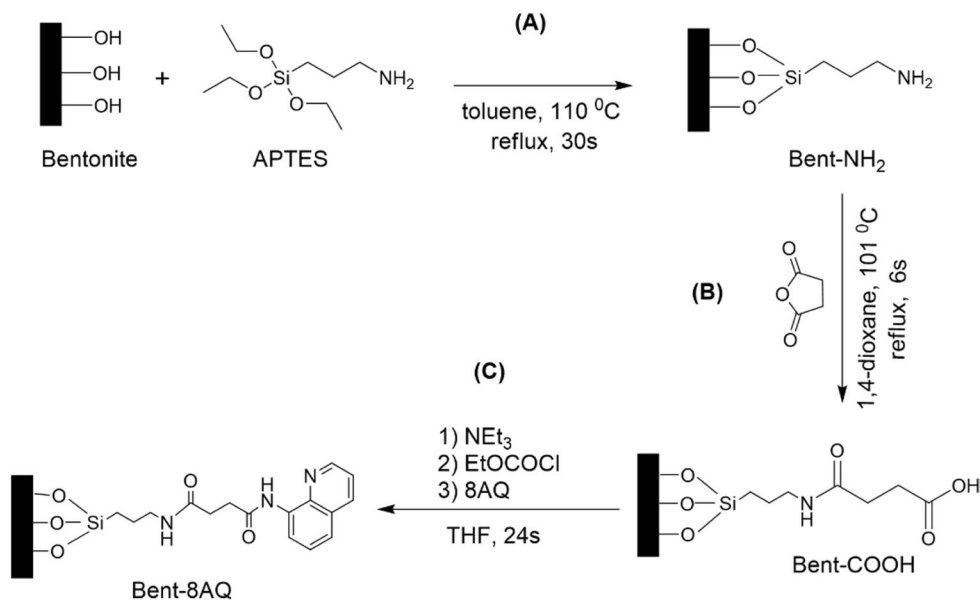
out by a Orion Star A211 (Thermo Scientific) Bench top pH meter.

Functionalization of bentonite For the obtainment of aminated bentonite (Bent-NH$_2$) (Scheme 1-(A)), the synthesis procedure described in the previous research was followed [48]. For this, 6 cm^3 (25.6 mmol, 5.68 g) of APTES ((3-aminopropyl)triethoxysilane)) was dissolved in 60 cm^3 of anhydrous toluene and then 5 g of bentonite was added into this mixture. The resultant mixture was refluxed at 110 °C for 30 h under N$_2$ atmosphere. At the end of the period of 30 h, when the reaction flask was cooled, the solid material in the reaction flask was filtered off. After the solid material was dried in an oven at 80 °C for 24 h, an off-white substance was obtained.

For the preparation of Bent-COOH (Scheme 1-(B)) from the starting material of Bent-NH$_2$, the synthesis procedure suggested in a previous study was pursued [30]. For this purpose, 2 g of Bentonite-NH$_2$ were dispersed in 60 cm^3 of 1,4-dioxane and 2 g of succinic anhydride was incorporated into the mixture. After the pH of the mixture was adjusted to 4.0, it was refluxed at 101 °C for 6 h. After the 6 h period has elapsed, the reaction flask was cooled to room temperature, and the solid in 1,4-dioxane was separated by filtration over a Teflon membrane filter. After the filtrated solid material was dried in an oven at 80 °C for 24 h, a white solid of 2.13 g was obtained.

For the amidation reaction of the Bent-COOH (Scheme 1-(C)), the similar procedure with a slight modification was followed [30]. The mixture prepared by dispersing 1.5 g of Bentonite-COOH in 50 cm^3 of THF in a 100 cm^3 reaction balloon was cooled to 0 °C and 96 mg of NEt$_3$ (0.945 mmol)

was added dropwise into this mixture. In follow, 103 mg of EtOCOCl (0.945 mmol) was added dropwise into the same mixture and the resultant mixture was stirred at 0 °C for 30 min. After the time period of 30 min, 136 mg of 8-aminoquinoline (0.94 mmol) was annexed to this mixture, and the mixture was stirred for more 1 h at 0 °C. Later, after the temperature of the mixture was reached to room temperature, the mixture was stirred at room temperature for extra 24 h. Finally, the solid material in THF was filtered through a Teflon membrane filter and left to dry in an oven at 80 °C for 24 h. The resulting solid (Bent-8AQ) was obtained as 1.55 g.

Fabrication of PVC-membrane electrode and measurement procedure In the fabrication of the electrode the procedures described in our previous studies were traced [29, 30]. The electrode manufacturing process usually consisted of two stages. In the first step, solid-contact preparation to obtain conductive interfaces compatible with the PVC film coating is performed. Solid contacts are prepared by immersing the bare end of a copper wire in a homogeneous mixture of 50% (w/w) graphite, 35% (w/w) epoxy, and 15% (w/w) hardener in THF and dried at room temperature overnight. In the second step, a membrane cocktail of the appropriate composition was prepared and applied to the solid-contact surface obtained in the first step. PVC membranes covered on solid-contact surfaces at miscellaneous compositions were prepared by dissolving 100 mg of total membrane mass in 2 cm^3 of THF. Solid contact surfaces were submerged into the prepared PVC-membrane cocktails several times and the resultant surfaces were dried at least 12 h at ambient temperature (Scheme 2). The manufactured electrodes

Scheme2
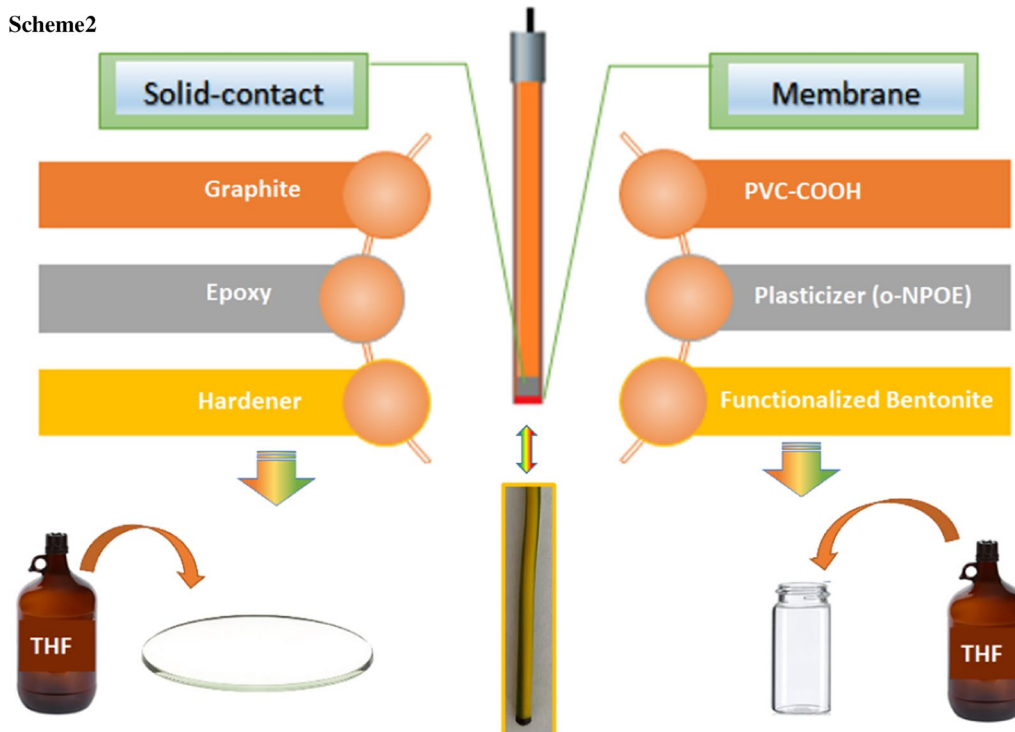
were conditioned by immersing into a 20 cm^3 10^{-3} mol/dm^3 Cu^{2+} solution for 12 h. The potentiometric cell assembly utilized in the current study can be represented schematically as follows:

Conductive wire │ solid-state contact │ Cu^{2+}-selective carboxylated-PVC membrane │ test solution │ saturated Hg/Hg$_2$Cl$_2$ reference electrode.

References

1. Kaur I, Sharma M, Kaur S, Kaur A (2020) Sens Actuators B: Chem 312:127935
2. Paul A, Nair RR, Chatterjee PB, Srivastava DN (2018) ACS Omega 3:16230
3. Maiti S, Prasad B, Minocha AK (2020) SN Appl Sci 2:2151
4. Pierson H, Yang H, Lutsenko S (2019) Annu Rev Nutr 39:75
5. Uauy R, Olivares M, Gonzalez M (1998) Am J Clin Nutr 67:952S
6. Kapoor N, Shetty S, Thomas N, Paul TV (2014) Indian J Endocrinol Metab 18:855
7. Zhao C, Liu B, Bi X, Liu D, Pan C, Wang L, Pang Y (2016) Sens Actuators B: Chem 229:131
8. World Health Organization (WHO) (2011) Guidelines for drinking water quality, (4th edn)
9. Honorato FA, Honorato RS, Pimentel MF, Araujo MCU (2002) Analyst 127:1520
10. Zhong WS, Ren T, Zhao LJ (2016) J Food Drug Anal 24:46
11. Divrikli U, Kartal AA, Soylak M, Elci L (2007) J Hazard Mater 145:459
12. Jurado JM, Martin MJ, Pablos F, Moreda-Pineiro A, Bermejo-Barrera P (2007) Food Chem 101:1296
13. Ghaebi M, Saadati M (2016) J Radiat Nucl Technol 1:29
14. Hua Z (2021) China International Conference on Electricity Distribution (CICED) 235
15. Xiong H, Wang B, Wen W, Zhang X, Wang S (2019) Microchim Acta 186:392
16. Wainwright P, Wadey D, Cook P (2018) Ann Clin Biochem 55:485
17. Manousi N, Isaakidou E, Zachariadis GA (2022) Appl Sci 12:534
18. Akhond M, Absalan G, Pourshamsi T, Ramezani AM (2016) Talanta 154:461
19. Cattalini JP, Mouriño VS, Lucangioli SE (2016) Anal Methods 8:7767
20. Del Castillo Busto ME, Cuello-Nunez S, Ward-Deitrich C, Morley T, Goenaga-Infante H (2022) Anal Bioanal Chem 414:561
21. Yu H, Xu P, Lee D-W, Li X (2013) J Mater Chem A 1:4444
22. Mirceski V, Gulaboski R, Lovric M, Bogeski I, Kappl R, Hoth M (2013) Electroanalysis 25:2411
23. Pietrzak K, Wardak C, Cristóvão B (2022) Ionics 28:2423
24. El Badry MM, Frag EY, El Brawy MH (2021) Microchem J 164:106065
25. Kanberoglu GS, Coldur F, Topcu C, Cubuk O (2015) IEEE Sens J 15:6199
26. Zahran EM, New A, Gavalas V, Bachas LG (2014) Analyst 139:757
27. Paczosa-Bator B, Piech R, Lewenstam A (2010) Talanta 81:1003
28. Radu A, Anastasova-Ivanova S, Paczosa-Bator B, Danielewski M, Bobacka J, Lewenstam A, Diamond D (2010) Anal Methods 2:1490
29. Topcu C, Caglar B, Guner EK, Coldur F, Caglar S, Yıldırım O, Ozdokur KV, Cubuk O (2019) Anal Lett 52:2524

30. Topcu C, Caglar S, Caglar B, Coldur F, Cubuk O, Sarp G, Gedik K, Cirak BB, Tabak A (2016) Adv Nat Sci: Nanosci Nanotechnol 7:035012

31. Prasad K, Kala R, Prasada Rao T, Naidu GRK (2006) Anal Chim Acta 566:69

32. Abdel-Haleem F, Mahmoud S, Abdel-Ghani NET, El Nashar RM, Bechelany M, Barhaum A (2021) Sensors 21:3150

33. Gad ES, Ali TA, Elsayed AA-E, Mohamed GG, El-Bary HA (2020) Int J Electrochem Sci 15:11904

34. Caglar B, Cubuk O, Demir E, Coldur F, Catir M, Topcu C, Tabak A (2015) J Mol Struct 1089:59

35. Chipera SJ, Bish DL (2001) Clays Clay Miner 49:398

36. Caglar B, Keles Guner E, Ersoy S, Caglar S, Ozdemir AO, Ozdokur KV, Dogan B, Icer F, Cirak C (2021) J Alloys Compd 885:160964

37. Guo Y, Gong Z, Li P, Zhang W, Gao B (2016) Ceram Int 42:8850

38. Buck RP, Lindner E (1994) Pure Appl Chem 66:2527

39. Umezawa Y, Buhlmann P, Umezawa K, Tohda K, Amemiya S (2000) Pure Appl Chem 72:1851

40. Tutulea-Anastasiu MD, Wilson D, Del Valle M, Schreiner CM, Cretescu I (2013) Sensors 13:4367

41. Hasani B, Zamani A, Moftakhar MK, Mostafavi M, Yaftian MR, Ghorbanloo M (2018) J Anal Chem 73:82

42. Kumar DM, Suresh J, Neeraj J, Poonam B (2013) Res J Chem Environ 17:82

43. Kamel AH, Mahmoud WH, Mostafa MS (2010) Electroanalysis 22:2453

44. Akhond M, Ghaedi M, Tashkhourian J (2005) Bull Korean Chem Soc 26:882

45. Abu-Dalo MA, Salam AA, Nassory NS (2015) Int J Electrochem Sci 10:6780

46. Gupta VK, Singh LP, Singh R, Upadhyay N, Kaur SP, Sethi B (2012) J Mol Liq 174:11

47. Singh LP, Bhatnagar JM (2004) Talanta 64:313

48. Anirudhan TS, Jalajamony S, Sreekumari SS (2012) Appl Clay Sci 65–66:67